Results

Clinical characteristics

Table 1 shows the baseline characteristics and treatment regimens of 70 patients with PAH-CTD. Almost half of patients were referred because of a suspicion of PAH. In the others, PAH was diagnosed during regular follow-up at a rheumatology clinic. MCTD was the most common underlying CTD (43%), followed by SLE (29%), SSc (19%) and primary SS (10%). Eleven (85%) of the 13 SSc patients with PAH were classified as having lcSSc. The most prevalent ANA was anti-U1RNP antibody (61%). Anti-SSA antibody was detected in 38 patients (54%), including 6 in whom the anti-SSA antibody with or without anti-SSB antibody was the only known ANA specificity. In contrast, the prevalence of ACA was only 16%. At the time of PAH diagnosis, 69% of patients were classified as WHO-FC III or IV, with moderately or severely impaired haemodynamics. At least one PAH drug was administered to 56% of the patients immediately after the diagnosis of PAH, and 41% received a sequential combination therapy consisting of two or three PAH drugs. Immunosuppressive treatment was given to 37% of the patients at the time of PAH diagnosis. Seventeen patients (27%) had radiological evidence of ILD, but all of them presented with minimal disease activity on imaging and normal or slightly depressed restrictive ventilatory function (FVC $\geqslant$70%).

Comparison of the baseline characteristics between the historical and recent groups (Table 1) revealed a greater frequency of referral in recent cases ($P = 0.001$), an older age at PAH diagnosis ($P < 0.001$), a lower frequency of RP ($P < 0.001$) and a higher frequency of ILD ($P = 0.04$). The haemodynamic parameters tended to be worse in recent cases than in historical ones. Finally, as expected, at least one PAH drug was administered to all except one recent patient, whereas none were administered to historical patients ($P < 0.001$).

Table 1 Demographic and clinical characteristics at PAH diagnosis and treatment regimens for patients with PAH-CTD

Demographic and clinical features	All patients ($n = 70$)	Historical group ($n = 30$)	Recent group ($n = 40$)	P[a]
Referral patients (%)	49	27	65	0.001
Female (%)	100	100	100	1.0
Age at PAH diagnosis (years)	40 (16)	31 (10)	47 (17)	<0.001
Time between CTD onset and PAH diagnosis (months)	74 (89)	35 (32)	103 (106)	0.03
RP (%)	74	97	58	<0.001
ILD (%)	27	13	38	0.04
Pericardial effusion (%)	24	20	28	0.7
Renal disorder (%)	7	3	10	0.4
Underlying CTD (%)				
MCTD	43	63	28	0.08
SLE	29	20	35	
SSc	19	13	23	
Primary SS	10	3	15	
ANA (%)				
Anti-U1RNP	61	70	56	0.3
Anti-Sm	16	13	18	0.9
Anti-SSA	54	67	45	0.07
Anti-SSB	20	23	18	0.8
Anticentromere	16	7	23	0.1
Anti-topo I	1	0	3	1.0
Anti-double-stranded DNA	23	17	28	0.4
WHO-FC (%)				
Class I	3	0	5	0.3
Class II	29	30	28	
Class III	56	47	63	
Class IV	13	23	5	
Haemodynamic parameters				
mPAP, mmHg	45 (12)	42 (14)	47 (10)	0.06
CO, l/min	3.7 (1.1)	4.0 (1.0)	3.6 (1.2)	0.07
PVR, Wood units	11.6 (6.0)	9.9 (5.8)	12.9 (6.0)	0.02
Treatment regimen (%)				
At least one PAH drug	56	0	98	<0.001
Immunosuppressive treatment	37	43	33	0.4

Values are presented as the mean (S.D.), unless otherwise indicated. [a]Comparisons between historical and recent groups.

TABLE 2 Demographic and clinical characteristics at PAH diagnosis in patients with MCTD, SLE, SSc and primary SS

Demographic and clinical features	MCTD ($n=30$)	SLE ($n=20$)	SSc ($n=13$)	Primary SS ($n=7$)	Overall P
Age at PAH diagnosis (years)	37 (12)	32 (12)	56 (13)	50 (20)	<0.001[a]
Time between CTD onset and PAH diagnosis (months)	51 (56)	88 (107)	116 (110)	56 (91)	0.2
RP (%)	97	45	92	29	<0.001[b]
ILD (%)	33	10	31	43	0.4
Pericardial effusion (%)	27	35	15	0	0.6
Renal disorder (%)	0	25	0	0	0.03[c]
ANA (%)					
Anti-U1RNP	100	55	8	14	<0.001[d]
Anti-Sm	27	15	0	0	0.3
Anti-SSA	63	60	8	86	<0.001[e]
Anti-SSB	27	20	0	29	0.4
Anti-centromere	0	10	60	14	<0.001[f]
Anti-topo I	0	0	8	0	0.5
Anti-double-stranded DNA	17	50	8	0	0.03[g]
WHO-FC (%)					
Class I	0	10	0	0	1.0
Class II	30	20	39	29	
Class III	57	60	46	57	
Class IV	13	10	15	14	
Haemodynamic parameters					
mPAP, mmHg	41 (11)	48 (11)	44 (14)	51 (11)	0.08
CO, l/min	3.8 (1.1)	3.9 (1.3)	3.6 (1.1)	3.1 (0.5)	0.5
PVR, Wood units	10.3 (5.8)	12.2 (5.2)	12.0 (7.6)	15.4 (5.2)	0.1

Values are presented as the mean (S.D.), unless otherwise indicated. Significant differences (overall $P<0.05$) were further analysed by pairwise comparisons. [a]$P<0.01$ between MCTD and SLE, SSc or primary SS, and between SLE and SSc; $P=0.04$ between SLE and primary SS. [b]$P<0.01$ between MCTD and SLE or primary SS, between SLE and SSc, and between SSc and primary SS. [c]$P<0.01$ between SLE and MCTD. [d]$P<0.01$ between MCTD and SLE, SSc or primary SS, and between SLE and SSc. [e]$P<0.01$ between MCTD, SLE or primary SS and SSc. [f]$P<0.01$ between MCTD or SLE and SSc. [g]$P<0.05$ between SLE and MCTD, SSc or primary SS.

Clinical features associated with underlying CTDs

Baseline demographic, clinical and haemodynamic parameters were compared according to underlying CTD (Table 2). Among the four CTD groups, patients with SLE were the youngest at PAH diagnosis, and MCTD patients were the next youngest, compared with patients with SSc or primary SS. RP was observed in nearly all patients with MCTD or SSc but in only 45% and 29% of patients with SLE and primary SS, respectively. Renal disorder was exclusively found in patients with SLE at diagnosis of PAH. The distribution of ANAs corresponded well with the individual CTDs. Anti-U1RNP antibody was predominantly found in MCTD and SLE, whereas anti-SSA antibody was detected broadly in non-SSc CTDs. ACA was the predominant ANA in SSc. There were no statistically significant differences in the WHO-FC or haemodynamic parameters among the four groups.

Survival rates

Cumulative survival rate was significantly better in the 40 recent cases than in the 30 historical ones ($P=0.003$; Fig. 1A), indicating that prognosis has improved in Japanese patients with PAH-CTD. All the deaths were related to PAH, and causes of death included PAH crisis, right heart failure and sudden death probably due to arrhythmia. The 1-, 3- and 5-year survival rates were 73%, 22% and 22%, respectively, in the historical group, and 87%, 76% and 53%, respectively, in the recent group. Differences in the cumulative survival rate among patients with MCTD, SLE, SSc and primary SS were not statistically significant (Fig. 1B) but there was a trend towards a worse survival rate in SSc patients, compared with patients with all the other CTDs combined, in the recent group ($P=0.08$).

Prognostic factors

To identify variables that predict outcomes at 1, 3 and 5 years after the PAH diagnosis in patients with PAH-CTD, we first performed a univariate analysis to find prognostic factors from the baseline characteristics and treatment regimens. An older age at PAH diagnosis and WHO-FC III/IV were associated with poor survival rates, whereas the use of any PAH drug was positively associated with survival at 1, 3 or 5 years. Additionally, a lower cardiac output (CO) and higher pulmonary vascular resistance (PVR) were associated with poor survival rates at 1 year and ILD with poor survival rates at 3 years. None of the underlying CTDs or ANAs were found to be a prognostic factor.

FIG. 1 Cumulative survival rates in 70 patients with PAH-CTD.

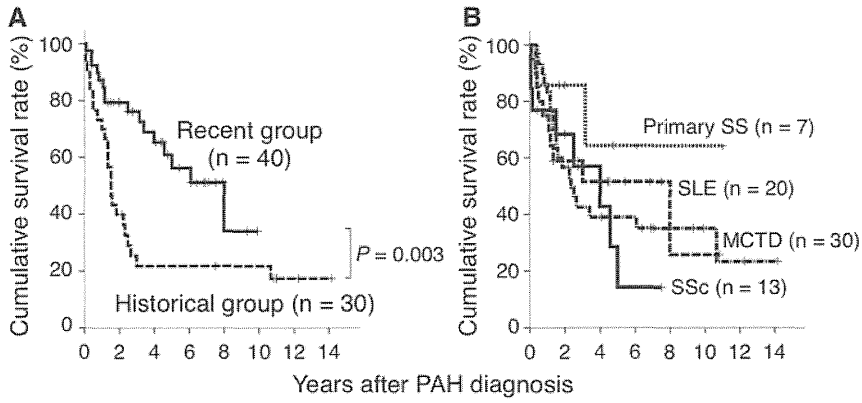

(**A**) The cumulative survival rates of the recent group and the historical group were compared. (**B**) The cumulative survival rates of the two groups were compared according to underlying CTD: MCTD, SLE, SSc or primary SS. Comparisons between the two groups were made using the log-rank test.

TABLE 3 Independent predictors of mortality at 1, 3 and 5 years after PAH diagnosis, obtained by multivariate analysis

	1 year		3 years		5 years	
Selected variables	HR (CI)	*P*	HR (CI)	*P*	HR (CI)	*P*
Age at PAH diagnosis	1.01 (0.96, 1.07)	0.7	0.99 (0.96, 1.04)	0.9	1.00 (0.97, 1.04)	0.9
ILD	1.38 (0.34, 5.61)	0.7	1.25 (0.36, 4.39)	0.7	1.67 (0.58, 4.78)	0.3
WHO-FC III or IV	2.53 (0.24, 26.3)	0.4	8.80 (1.81, 42.8)	0.007	10.83 (2.73, 43.0)	0.001
CO	0.60 (0.15, 2.31)	0.5	0.81 (0.42, 1.60)	0.6	0.68 (0.35, 1.35)	0.3
PVR	1.07 (0.81, 1.39)	0.7	1.07 (0.88, 1.29)	0.5	1.03 (0.87, 1.23)	0.7
Use of any PAH drug	0.11 (0.02, 0.72)	0.02	0.12 (0.03, 0.40)	0.001	0.11 (0.04, 0.35)	<0.001

Variables selected by univariate analysis were then subjected to multivariate analysis to find independent factors that predicted an increased risk of mortality. As shown in Table 3, WHO-FC III/IV was identified as a prognostic factor for mortality at 3 and 5 years ($P = 0.007$ and 0.001, respectively). Additionally, the use of any PAH drug was a factor for favourable outcomes at 1, 3 and 5 years ($P = 0.02$, 0.001 and <0.001, respectively).

To confirm the impact of the WHO-FC at PAH diagnosis on survival rates, the cumulative survival rate was compared between patients with WHO-FC I/II and those with FC III/IV (Fig. 2). The cumulative survival rate was higher in patients with WHO-FC I/II ($P < 0.001$). The 1- and 3-year survival rates were 95% and 90%, respectively, in patients with WHO-FC I/II, compared with 73% and 37%, respectively, in those with WHO-FC III/IV. We further evaluated the impact of the treatment regimen on the outcome in patients with WHO-FC I/II and III/IV separately (Fig. 3). In patients with WHO-FC III/IV, the cumulative survival rates were significantly different in patients who were and were not treated with PAH drugs, but the difference in patients with WHO-FC I/II was not statistically significant. On the other hand, there was no difference in the survival rates of patients who received and did not receive immunosuppressive treatment, regardless of the WHO-FC.

Discussion

This study, conducted at a single specialized PH centre, is the largest cohort study of Japanese patients with PAH-CTD. We found that the characteristics of Japanese patients with PAH-CTD included high frequencies of MCTD and SLE as underlying CTD, and a high frequency of serum anti-U1RNP antibody. These features are in sharp contrast to cohort studies conducted in the USA and Europe, in which SSc patients were found to comprise >70% of the patients with PAH-CTD [4–7], and ACA was the most frequent ANA [8-12, 24]. It is possible that MCTD patients were categorized as having SSc in the USA and European cohorts, since whether MCTD is a distinct disease has been a matter of controversy [25]. However, the anti-U1RNP antibody was infrequent in patients with SSc-associated PAH in the studies conducted in the USA [8, 24].

The mean age at PAH diagnosis in Japan was 40, which was younger than the 49–56 year range reported for the US and European cohorts [4–7]. This difference might be explained by the higher frequencies of MCTD and SLE

FIG. 2 Cumulative survival rates in 70 patients with PAH-CTD, stratified by WHO-FC.

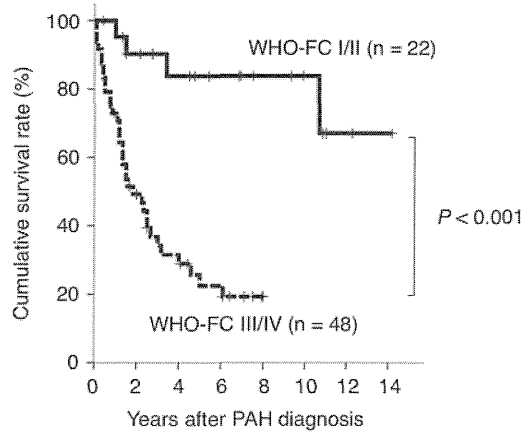

A comparison between groups was made using the log-rank test.

among the Japanese patients with PAH-CTD. Only a minor group of Japanese patients with PAH-CTD had SSc but these patients showed lcSSc, positive ACA and a relatively long disease duration at PAH diagnosis, which were all consistent with features reported in the USA and European patients with SSc-associated PAH [8, 26]. The distribution of underlying CTDs in our study was principally concordant with a recent study from northern Japan, which described a cohort of patients with PAH-CTD containing eight with SLE, four with MCTD, four with primary SS, three with SSc and one each with RA and DM [27]. Interestingly, reports from eastern Asian countries, including Taiwan and China, show a higher frequency of SLE than SSc as an underlying CTD for PAH [28, 29]. Additionally, PAH was reported as the third leading cause of death in Korean patients with SLE [30]. The reasons for these ethnic differences in the distribution of underlying CTDs in patients with PAH-CTD remain unclear but genetic and environmental factors may play a role.

It has been proposed that early detection and therapeutic intervention are important for improving the survival rates of patients with PAH [31]. In support of this idea, we identified WHO-FC III/IV at PAH diagnosis as an independent risk factor for mortality, as reported previously [5, 15, 24], although it is a subjective indicator. We did not observe an improvement in short-term outcomes in WHO-FC I/II patients treated with PAH drugs but this may have been due to the small number of patients. To achieve early detection within the better functional classes, it is essential to screen specific populations that are at high risk of PAH. Patients with SSc, especially lcSSc with long-standing RP, represent a high-risk group, with a 5–10% lifetime risk of developing symptomatic PAH [32]. Therefore, annual screening with echocardiography is recommended for such patients [33], although it has not been demonstrated yet as to which strategy would be cost effective. The same strategy might not be effective in Japan because SSc patients were not the only high-risk population. Moreover, 26% of patients with PAH-CTD did not have RP. Therefore, screening should be expanded to a broad panel of CTDs, including SLE and MCTD, although it is impractical to screen a large number of patients in clinical settings. Given this situation, the anti-U1RNP antibody is a potential hallmark for selecting the high-risk group. Further prospective studies are necessary to identify risk factors that predict the development of PAH in eastern Asian CTD patients, including Japanese, Chinese and Korean patients.

Survival rates were significantly better in recent cases compared with historical ones in our cohort, although baseline haemodynamics tended to be worse in the recent group. Additionally, the use of any PAH drug was an independent predictor for better survival rates. These results indicate that the prognosis of Japanese patients with PAH-CTD has improved in the modern treatment era. However, long-term survival rates were still disappointedly low even in the recent group: the 5-year survival rate was 53%. There are several possible reasons for this poor outcome. First, ~70% of patients already had advanced PAH with WHO-FC III/IV at their diagnosis. Moreover, all patients diagnosed before 2005 received monotherapy with either beraprost or epoprostenol as the first-line therapy. However, similar or even worse outcomes have been reported in recent cohorts of patients with SSc-associated PAH: the 3-year survival rate was 64% in the USA [12], 56% in France [15], 47% in the United Kingdom [5] and 39% in Sweden [11]. The prognosis of PAH is worse in patients with SSc than in those with non-SSc CTDs [5, 16] but the 3-year survival rate in a Chinese cohort that included significant proportions of patients with SLE or MCTD was as low as 54% [29]. Together, these findings indicate that patients with PAH-CTD have a poor prognosis, even in the era of modern PAH-CTD management.

Immunosuppressive treatment is effective for improving symptoms and haemodynamic parameters in some patients with PAH-CTD, especially in those with active-phase SLE or MCTD [27, 34, 35]. Despite these short-term effects, immunosuppressive treatment did not improve long-term survival in our cohort, which contained a high proportion of patients with MCTD and SLE. Therefore, it is likely that the effects of immunosuppressive treatment are limited and PAH drugs should be used in combination with immunosuppressive treatment for patients with PAH associated with MCTD or SLE.

Although this study provides important observations in terms of Japanese patients with PAH-CTD, referral bias should be considered as a potential limitation, since our hospital is the oldest specialized PH centre in the Tokyo metropolitan area. Nearly half of the patients in the present study were referred mainly by cardiologists or pulmonologists and had never received PAH screening. Therefore, the cases most likely to be referred were those with severe PAH and mild CTD-related symptoms. Detection of patients with mild or early PAH would be

FIG. 3 Cumulative survival rates in 70 patients with PAH-CTD, stratified by treatment regimen.

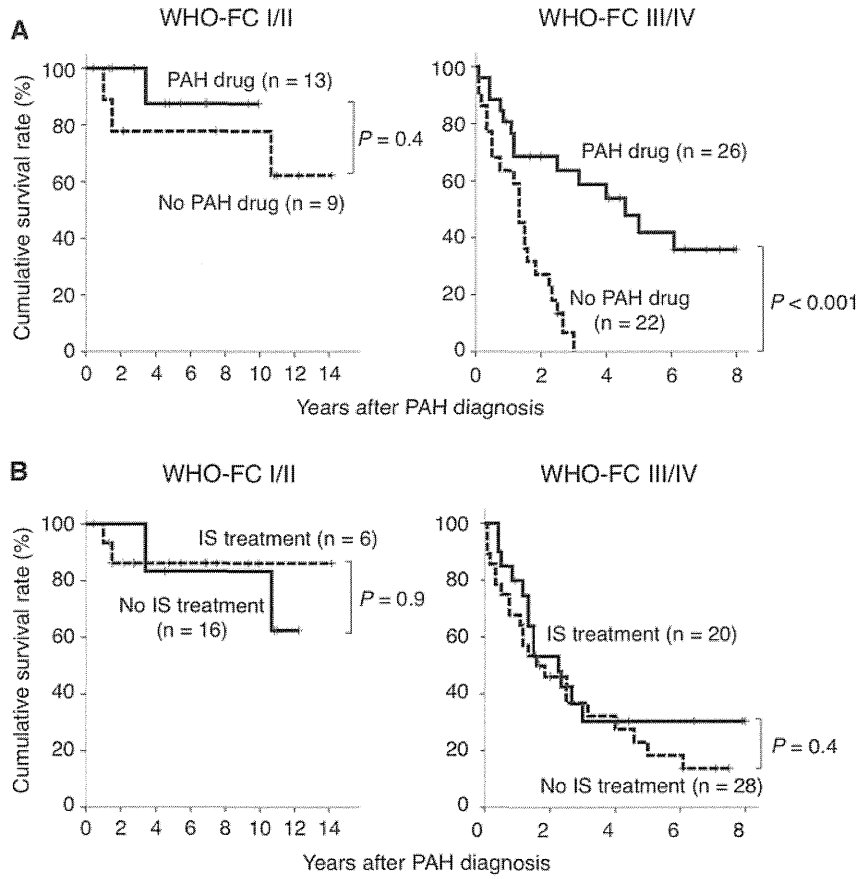

Comparisons were made in patients with WHO-FC I/II and those with WHO-FC III/IV separately. (**A**) The cumulative survival rate was compared between patients who received at least one PAH drug and those who did not. (**B**) The cumulative survival rate was compared between patients who received immunosuppressive (IS) treatment and those who did not. Comparisons between two groups were made using the log-rank test.

expected by a recent campaign aimed to promote the PAH screening of asymptomatic patients with CTD but the recent group included more referral patients than the historical group. This may explain the differences in the baseline characteristics of the historical and recent groups: the haemodynamics were more severe and the frequency of MCTD lower in the recent group. Additionally, as in studies carried out in other east Asian countries [27–30], a small number of the patients in our cohort may have been subject to selection bias. Therefore, the subjects in our study might not reflect the composition of the general PAH-CTD patient population in Japan. Another limitation of this study is the lack of male patients in the study population, since a recent study demonstrated potential differences in baseline haemodynamic characteristics and outcomes between men and women with PAH [36].

In summary, the underlying CTDs and ANA profiles in Japanese patients with PAH-CTD were apparently different from those in the USA and Europe. Modern PAH treatment improves survival rates, but long-term outcomes are still unsatisfactory. Early detection of PAH is important for further improving survival rates but a screening strategy specific to Japanese CTD patients needs to be developed.

Rheumatology key messages

- High frequencies of MCTD/SLE and anti-U1RNP antibody are hallmarks of PAH-CTD in Japanese patients.
- The prognosis of Japanese patients with PAH-CTD has improved with modern treatment.
- WHO-FC at baseline is an independent prognostic factor in Japanese patients with PAH-CTD.

Funding: This work was supported by a research grant for intractable diseases from the Japanese Ministry of Health, Labour and Welfare.

Disclosure statement: The authors have declared no conflicts of interest.

References

1 Koh ET, Lee P, Gladman DD *et al*. Pulmonary hypertension in systemic sclerosis: an analysis of 17 patients. Br J Rheumatol 1996;35:989–93.

2 Trad S, Amoura Z, Beigelman C *et al*. Pulmonary arterial hypertension is a major mortality factor in diffuse systemic sclerosis, independent of interstitial lung disease. Arthritis Rheum 2006;54:184–91.

3 Vegh J, Szodoray P, Kappelmayer J *et al*. Clinical and immunoserological characteristics of mixed connective tissue disease associated with pulmonary arterial hypertension. Scand J Immunol 2006;64:69–76.

4 Chung L, Liu J, Parsons L *et al*. Characterization of connective tissue disease-associated pulmonary arterial hypertension from REVEAL: identifying systemic sclerosis as a unique phenotype. Chest 2010;138:1383–94.

5 Condliffe R, Kiely DG, Peacock AJ *et al*. Connective tissue disease-associated pulmonary arterial hypertension in the modern treatment era. Am J Respir Crit Care Med 2009; 179:151–7.

6 Humbert M, Sitbon O, Chaouat A *et al*. Pulmonary arterial hypertension in France: results from a national registry. Am J Respir Crit Care Med 2006;173:1023–30.

7 Ruiz-Cano MJ, Escribano P, Alonso R *et al*. Comparison of baseline characteristics and survival between patients with idiopathic and connective tissue disease-related pulmonary arterial hypertension. J Heart Lung Transplant 2009;28:621–7.

8 Steen V, Medsger TA Jr. Predictors of isolated pulmonary hypertension in patients with systemic sclerosis and limited cutaneous involvement. Arthritis Rheum 2003;48: 516–22.

9 Mukerjee D, George D, Coleiro B *et al*. Prevalence and outcome in systemic sclerosis associated pulmonary arterial hypertension: application of a registry approach. Ann Rheum Dis 2003;62:1088–93.

10 Launay D, Humbert M, Berezne A *et al*. Clinical characteristics and survival in systemic sclerosis-related pulmonary hypertension associated with interstitial lung disease. Chest 2011;140:1016–24.

11 Hesselstrand R, Wildt M, Ekmehag B, Wuttge DM, Scheja A. Survival in patients with pulmonary arterial hypertension associated with systemic sclerosis from a Swedish single centre: prognosis still poor and prediction difficult. Scand J Rheumatol 2011;40:127–32.

12 Mathai SC, Hummers LK, Champion HC *et al*. Survival in pulmonary hypertension associated with the scleroderma spectrum of diseases: impact of interstitial lung disease. Arthritis Rheum 2009;60:569–77.

13 Kasukawa R, Nishimaki T, Takagi T *et al*. Pulmonary hypertension in connective tissue disease. Clinical analysis of sixty patients in multi-institutional study. Clin Rheumatol 1990;9:56–62.

14 Williams MH, Das C, Handler CE *et al*. Systemic sclerosis associated pulmonary hypertension: improved survival in the current era. Heart 2006;92:926–32.

15 Hachulla E, Carpentier P, Gressin V *et al*. Risk factors for death and the 3-year survival of patients with systemic sclerosis: the French ItinérAIR-Sclérodermie study. Rheumatology 2009;48:304–8.

16 Denton CP, Pope JE, Peter HH *et al*. Long-term effects of bosentan on quality of life, survival, safety and tolerability in pulmonary arterial hypertension related to connective tissue diseases. Ann Rheum Dis 2008;67:1222–8.

17 Badesch DB, Champion HC, Sanchez MA *et al*. Diagnosis and assessment of pulmonary arterial hypertension. J Am Coll Cardiol 2009;30:S55–66.

18 Denton CP, Humbert M, Rubin L, Black CM. Bosentan treatment for pulmonary arterial hypertension related to connective tissue disease: a subgroup analysis of the pivotal clinical trials and their open-label extensions. Ann Rheum Dis 2006;65:1336–40.

19 Hochberg MC. Updating the American College of Rheumatology revised criteria for the classification of systemic lupus erythematosus. Arthritis Rheum 1997;40: 1725.

20 Subcommittee for Scleroderma Criteria of the American Rheumatism Association Diagnostic and Therapeutic Criteria Committee: preliminary criteria for the classification of systemic sclerosis (scleroderma). Arthritis Rheum 1980;23:581–90.

21 Kasukawa R, Tojo T, Miyawaki S. Preliminary diagnostic criteria for classification of mixed connective tissue disease. In: Kasukawa R, Sharp GC, eds. Mixed connective tissue disease and antinuclear antibodies. Amsterdam: Elsevier, 1987:41–7.

22 Vitali C, Bombardieri S, Jonsson R *et al*. Classification criteria for Sjögren's syndrome: a revised version of the European criteria proposed by the American–European Consensus Group. Ann Rheum Dis 2002;61:554–8.

23 Kuwana M, Kaburaki J, Okano Y, Tojo T, Homma M. Clinical and prognostic associations based on serum antinuclear antibodies in Japanese patients with systemic sclerosis. Arthritis Rheum 1994;37:75–83.

24 Campo A, Mathai SC, Le Pavec J *et al*. Hemodynamic predictors of survival in scleroderma-related pulmonary arterial hypertension. Am J Respir Crit Care Med 2010; 182:252–60.

25 Smolen JS, Steiner G. Mixed connective tissue disease: to be or not to be? Arthritis Rheum 1998;41:768–77.

26 Medsger TA. Natural history of systemic sclerosis and the assessment of disease activity, severity, functional status, and psychologic well-being. Rheum Dis Clin North Am 2003;29:255–73.

27 Miyamichi-Yamamoto S, Fukumoto Y, Sugimura K *et al*. Intensive immunosuppressive therapy improves pulmonary hemodynamics and long-term prognosis in patients with pulmonary arterial hypertension associated with connective tissue disease. Circ J 2011;75:2668–74.

28 Chen CH, Chen HA, Wang HP *et al*. Pulmonary arterial hypertension in autoimmune diseases: an analysis of 19 cases from a medical center in northern Taiwan. J Microbiol Immunol Infect 2006;39:162–8.

29 Zhang R, Dai LZ, Xie WP *et al*. Survival of Chinese patients with pulmonary arterial hypertension in the modern management era. Chest 2011;140:301–9.

30 Kim WU, Min JK, Lee SH, Park SH, Cho CS, Kim HY. Causes of death in Korean patients with systemic lupus erythematosus: a single center retrospective study. Clin Exp Rheumatol 1999;17:539–45.

31 Lau EM, Manes A, Celermajer DS, Galiè N. Early detection of pulmonary vascular disease in pulmonary arterial hypertension: time to move forward. Eur Heart J 2011;32:2489–98.

32 Avouc J, Airo P, Meune C *et al*. Prevalence of pulmonary hypertension in systemic sclerosis in European Caucasians and metaanalysis of 5 studies. J Rheumatol 2010;37:2290–8.

33 Hachulla E, Gressin V, Guillevin L *et al*. Early detection of pulmonary arterial hypertension in systemic sclerosis: a French nationwide prospective multicenter study. Arthritis Rheum 2005;52:3792–800.

34 Sanchez O, Stibon O, Jais X, Simonneau G, Humbert M. Immunosuppressive therapy in connective tissue diseases-associated pulmonary arterial hypertension. Chest 2006;130:182–9.

35 Kato M, Kataoka H, Odani T *et al*. The short-term role of corticosteroid therapy for pulmonary arterial hypertension associated with connective tissue diseases: report of five cases and a literature review. Lupus 2011;20:1047–56.

36 Shapiro S, Traiger GL, Turner M, McGoon MD, Wason P, Barst RJ. Sex differences in the diagnosis, treatment, and outcome of patients with pulmonary arterial hypertension enrolled in the registry to evaluate early and long-term pulmonary arterial hypertension management. Chest 2012;141:363–73.

ARTHRITIS & RHEUMATISM
Vol. 64, No. 11, November 2012, pp 3726–3735
DOI 10.1002/art.34643

Potential Roles of Interleukin-17A in the Development of Skin Fibrosis in Mice

Yoshinobu Okamoto,[1] Minoru Hasegawa,[1] Takashi Matsushita,[1] Yasuhito Hamaguchi,[1] Doanh Le Huu,[1] Yoichiro Iwakura,[2] Manabu Fujimoto,[1] and Kazuhiko Takehara[1]

Objective. **Although transforming growth factor β (TGFβ) and connective tissue growth factor (CTGF) have been considered to play central roles in the pathogenesis of systemic sclerosis (SSc), other cytokines may also be crucial for the development of SSc. The aim of this study was to examine the roles of T helper cytokines in the development of skin fibrosis.**

Methods. **To compare the roles of Th1, Th2, and Th17 cytokines, we examined bleomycin-induced SSc in mice deficient for interferon-γ (IFNγ), interleukin-4 (IL-4), and IL-17A. The mechanism by which IL-17A contributes to bleomycin-induced fibrosis was investigated in vivo and in vitro. The outcome of mice lacking IL-17A was also investigated in TSK-1 mice.**

Results. **The loss of IL-17A significantly attenuated bleomycin-induced skin fibrosis, whereas a deficiency of IFNγ or IL-4 did not. Leukocyte infiltration and the expression of TGFβ and CTGF messenger RNA in bleomycin-injected skin were significantly reduced in IL-17A–deficient mice compared with wild-type (WT) mice. Daily bleomycin injections induced the expression of IL-17A in the skin and potent IL-17A producers in splenic CD4+ T cells from WT mice. Furthermore, a skin fibroblast cell line expressed increased TGFβ, CTGF, and collagen after the addition of recombinant IL-17A. IL-17A deficiency also attenuated skin thickness in TSK-1 mice.**

Conclusion. **This study demonstrates that IL-17A contributes to skin fibrosis in 2 mouse models of SSc. These findings suggest that inhibition of IL-17A represents a therapeutic target for antagonizing fibrotic skin disorders such as SSc.**

Systemic sclerosis (SSc) is an autoimmune connective tissue disease characterized by excessive extracellular matrix deposition in the skin, lungs, and other internal organs (1,2). A growing body of evidence suggests that overproduction of extracellular matrix components by activated fibroblasts results from complex interactions between various cells, including leukocytes and fibroblasts, and via several soluble mediators, such as cytokines, chemokines, and growth factors (1,2).

An emerging hypothesis for the pathogenesis of fibrotic disorders suggests that an imbalance between Th1 cytokines and Th2 cytokines leads to abnormal responses to tissue injury. Th2 cytokines such as interleukin-4 (IL-4), IL-6, and IL-13 stimulate the synthesis of collagen by human fibroblasts (3). In contrast, Th1 cytokines such as interferon-γ (IFNγ) and tumor necrosis factor α suppress collagen production by fibroblasts in vitro (3). Therefore, in general, a relative shift toward Th2 cytokine production rather than Th1 cytokine production can induce tissue fibrosis.

In patients with SSc, circulating T cells and T cells infiltrating the skin or lungs demonstrate a predominantly Th2 profile (4–6). Furthermore, a recent study suggested that the frequency of circulating Th17 cells is strikingly increased in patients with SSc (7). Th17 cells, which were discovered in 2007, are the third T helper cell subset that can produce IL-17A (8,9). Th17 cells also secrete IL-17F, IL-21, and IL-22. The differentiation factors transforming growth factor β (TGFβ) plus IL-6

Supported by grants-in-aid from the Ministry of Education, Science, and Culture of Japan, Research of Intractable Diseases grants from the Ministry of Health, Labor, and Welfare of Japan, Core Research for Evolutional Science and Technology program grants from the Japan Science and Technology Agency, and grants from the Bio-oriented Technology Research Advancement Institution.

[1]Yoshinobu Okamoto, MD, Minoru Hasegawa, MD, Takashi Matsushita, MD, PhD, Yasuhito Hamaguchi, MD, PhD, Doanh Le Huu, MD, Manabu Fujimoto, MD, Kazuhiko Takehara, MD, PhD: Kanazawa University Graduate School of Medical Science, Kanazawa, Japan; [2]Yoichiro Iwakura, MD, PhD: University of Tokyo, Tokyo, Japan.

Address correspondence to Minoru Hasegawa, MD, Department of Dermatology, Kanazawa University Graduate School of Medical Science, 13-1 Takaramachi, Kanazawa, Ishikawa 920-8641, Japan. E-mail: minoruha@derma.m.kanazawa-u.ac.jp.

Submitted for publication February 5, 2012; accepted in revised form July 17, 2012.

or IL-21, the growth and stabilization factor IL-23, and the transcription factors RORγt, RORα, and STAT-3 have been considered to be involved in the development of Th17 cells. This T helper cell subset may contribute not only to inflammation but also to fibrosis via production of IL-17A and other cytokines (10). In fact, elevated serum IL-17A levels and augmented IL-17A expression in peripheral blood lymphocytes and lesional skin have been reported in patients with SSc (7,11,12), although reduced plasma IL-17A levels were detected in a recent study (13).

Skin fibrosis induced by daily intradermal bleomycin injections is widely used as a representative animal model of SSc (14). Although a variety of factors have been reported to contribute to the fibrotic process, the exact mechanism remains unclear. In a previous study, administration of recombinant IFNγ, a representative Th1 cytokine, attenuated bleomycin-induced skin fibrosis (15). IFNγ-deficient mice have modest bleomycin-induced lung fibrosis (16). IL-4 signaling has been reported as critical for the development of increased skin thickness in the TSK-1 (TSK/+) mouse model, a genetic model of SSc (17,18). In contrast, IL-4 is not required for the development of bleomycin-induced lung fibrosis (19). However, both bleomycin- and IL-1β–induced lung fibrosis are dependent on IL-17A (10). The specific roles of IFNγ, IL-4, and IL-17A in bleomycin-induced skin fibrosis have not been investigated using mice deficient for each of these cytokines.

In the current study, we demonstrated that IL-17A, but not IFNγ or IL-4, has pivotal roles in the development of skin fibrosis in a murine model of bleomycin-induced skin fibrosis. Furthermore, skin thickness was attenuated by IL-17A deficiency in TSK/+ mice, another model of skin fibrosis (20).

MATERIALS AND METHODS

Mice. IFNγ$^{-/-}$, IL-4$^{-/-}$, and IL-17A$^{-/-}$ mice (C57BL/6 genetic background) were generated as previously reported (21–23). These mice were all backcrossed at least 8 generations to C57BL/6 mice. TSK/+ mice (C57BL/6 background) and C57BL/6 mice were purchased from The Jackson Laboratory. IL-17A$^{-/-}$ TSK/+ mice were generated by crossing IL-17A$^{+/-}$ TSK/+ parents. To verify the TSK/+ genotype, polymerase chain reaction (PCR) amplification of a partially duplicated fibrillin 1 gene was carried out using genomic DNA from each mouse, as previously described (18). All mice were screened regularly for pathogens. Female mice ages 10 to 12 weeks were used for the experiments. The Committee on Animal Experimentation of Kanazawa University Graduate School of Medical Science approved all studies and procedures.

Intradermal bleomycin treatment. Bleomycin was dissolved in sterile saline at a concentration of 1 mg/ml. The mice received daily intradermal injections of either bleomycin or saline (300 μl, administered using a 27-gauge needle) into their shaved backs (the para-midline, lower back region) for 4 weeks, as described previously (14).

Histologic examination of skin fibrosis. All skin sections were obtained from the bleomycin-injected region of the lower back, as full-thickness sections extending down to the body wall musculature. The skin samples were fixed in formalin, dehydrated, embedded in paraffin, and used for immunostaining. Sections (6-μm thick) were stained with hematoxylin and eosin, Masson's trichrome, or van Gieson's reagents to identify collagen deposition in the skin. Expression of α-smooth muscle actin (α-SMA) was analyzed in paraffin-embedded specimens. After deparaffinization, samples were incubated with 3% H_2O_2. Positivity for α-SMA in mouse skin sections was detected by incubation with anti–α-SMA monoclonal antibodies conjugated to alkaline phosphatase (Sigma-Aldrich). Expression of the α-SMA was visualized with a New Fuchsin Substrate System (Dako). Skin thickness and the number of myofibroblasts (α-SMA–positive fibroblasts) were evaluated independently by 2 investigators (YO and MH), in a blinded manner. Fibroblasts were identified by their spindle-shaped morphology. The FreeHand tool of Adobe Photoshop Elements 3.0 was used to quantify specific van Gieson's staining in the skin sections.

Measurement of collagen content in tissue samples. Tissue samples were embedded in paraffin, and ~15-μm–thick sections were obtained. Sections were deparaffinized after incubation with xylol, xylol:ethanol (1:1), ethanol, water: ethanol (1:1), and water. Individual samples were placed in small test tubes and covered with 0.2 ml of a saturated solution of picric acid in distilled water that contained 0.1% fast green FCF and 0.1% sirius red F3BA. The samples were rinsed several times with distilled water until the fluid was colorless. One milliliter of 0.1N NaOH in absolute methanol (1:1 volume:volume) was added, and the eluted color was read on a spectrophotometer at 540 nm and 605 nm. The method used is based on the selective binding of sirius red F3BA and fast green FCF to collagens and noncollagenous proteins, respectively (24).

Immunohistochemical staining. Tissues were harvested prior to and on days 7, 14, 21, and 28 of bleomycin treatment; the numbers of infiltrating T cells, macrophages, and neutrophils were assessed by immunostaining. Deparaffinized sections were incubated with 3% H_2O_2. Sections were then incubated with rat monoclonal antibodies specific for CD3 (Serotec) or F4/80 (Abcam), or rabbit monoclonal antibodies specific for myeloperoxidase (MPO; NeoMarkers). Rat IgG (SouthernBiotech) was used as a control for nonspecific staining. Sections were then incubated sequentially (30 minutes at room temperature) with a biotinylated rabbit anti-rat IgG secondary antibody (BD Biosciences) or a biotinylated goat anti-rabbit IgG secondary antibody (Santa Cruz Biotechnology), followed by horseradish peroxidase–conjugated avidin–biotin complexes (Vectastain). Sections were washed 3 times with phosphate buffered saline (PBS) between incubations, developed with 3,3′-diaminobenzidine tetrahydrochloride dihydrate and hydrogen peroxide, and counterstained with methyl green. Each section was examined independently by

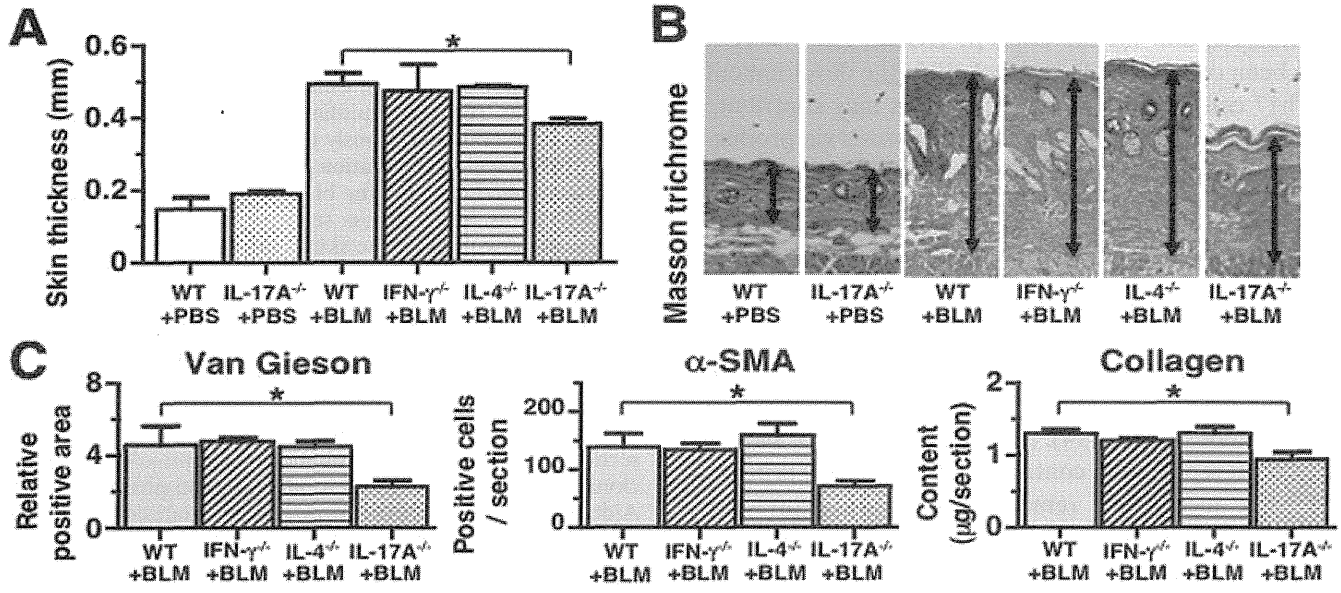

Figure 1. Skin fibrosis induced by intradermal bleomycin injections. Interferon-γ–deficient (IFNγ$^{-/-}$) mice, interleukin-4–deficient (IL-4$^{-/-}$) mice, IL-17A$^{-/-}$ mice, and wild-type (WT) mice were treated with daily intradermal injections of bleomycin (BLM) for 28 days. **A,** Dermal thickness. **B,** Representative images of skin tissue stained with Masson's trichrome. **Arrows** indicate skin thickness. Original magnification × 40. **C,** Histologic evaluation of skin fibrosis. Left, Size of fibrotic areas, as evaluated by van Gieson's staining. Middle, Number of α-smooth muscle actin (α-SMA)–positive fibroblastic cells. Right, Collagen content in lesional skin tissue sections. Bars show the mean ± SEM (n = 10 mice in each group). * = $P < 0.05$. PBS = phosphate buffered saline.

2 investigators (YO and MH), in a blinded manner, and the mean value was used for analysis.

Reverse transcriptase–PCR (RT-PCR). Skin was harvested 7 days after intradermal bleomycin treatment. Total RNA was isolated from frozen skin specimens using RNeasy spin columns (Qiagen) and was digested with DNase I (Qiagen) to remove chromosomal DNA, in accordance with the manufacturer's protocols. Total RNA was reverse transcribed to complementary DNA using a reverse transcription system with random hexamers (Promega). Cytokine messenger RNA (mRNA) was analyzed using real-time PCR quantification, according to the manufacturer's instructions (Applied Biosystems). Sequence-specific primers and probes were designed using predeveloped TaqMan assay reagents (Applied Biosystems). Real-time PCR (40 cycles of denaturation at 92°C for 15 seconds and annealing at 60°C for 60 seconds) was performed on an ABI Prism 7000 sequence detector (Applied Biosystems). GAPDH was used to normalize mRNA. Relative expression of real-time PCR products was determined by using the ΔΔCt method (25) to compare target gene and GAPDH mRNA expression. One of the control samples was chosen as a calibrator sample.

Cytokine concentrations in tissue. Samples of regional skin were homogenized in 600 μl of lysis buffer (10 mmoles/liter PBS, 0.1% sodium dodecyl sulfate, 1% Nonidet P40, 5 mmoles/liter EDTA containing complete protease inhibitor mixture [Roche Diagnostics]) to extract proteins. Homogenates were centrifuged at 15,000 revolutions per minute for 15 minutes at 4°C to remove debris (26). The total protein concentration in supernatants was measured with a BCA Protein Assay Kit (ThermoFisher Scientific) and was equalized in each sample. The concentration of IL-17A in supernatants was measured by enzyme-linked immunosorbent assay (ELISA; R&D Systems), according to the manufacturer's instructions.

Th17 cell induction by bleomycin treatment. Splenocytes were harvested from wild-type (WT) mice, and CD4+ T cells were purified by negative selection using MACS technology (Miltenyi Biotec). For in vitro Th17 cell differentiation, CD4+ T cells were cultured with 20 ng/ml of recombinant IL-6 (BioLegend), 5 ng/ml of recombinant human TGFβ1 (BioLegend), 10 μg/ml of anti–IL-4 antibody (BioLegend), and 10 μg/ml of anti-IFNγ antibody (BioLegend), in combination with 3 μg/ml of anti-CD3 antibody (eBioscience) and 5 μg/ml of anti-CD28 antibody (BioLegend) for 96 hours at 37°C. To evaluate the effect of bleomycin in this process, bleomycin was added to the culture medium simultaneously.

Splenocytes were also harvested from WT mice that received intradermal injections of bleomycin for 7 days. Purified CD4+ T cells were cultured in 96-well flat-bottomed plates precoated with anti-CD3 antibody (3 μg/ml) plus anti-CD28 (5 μg/ml) for 48 hours at 37°C.

For intracellular IL-17A staining, cultured CD4+ T cells were stimulated with phorbol myristate acetate (50 ng/ml; Sigma-Aldrich), ionomycin (0.5 μg/ml; Sigma-Aldrich), and monensin (2 μ*M*; eBioscience) for 4 hours before flow cytometric analysis. Each specimen was stimulated in triplicate wells.

Flow cytometric analysis. For 2-color or 3-color immunofluorescence analyses, cultured T cells were stained with anti-CD4 antibody (BD Biosciences) and anti–IL-17A antibody (BD Biosciences). Cells with the forward and side light-scatter properties of lymphocytes were analyzed on a

FACScan flow cytometer (BD Biosciences). Stained cells were fixed and permeabilized using a Cytofix/Cytoperm kit (BD Biosciences), according to the manufacturer's instructions, and stained with phycoerythrin-conjugated mouse anti–IL-17A monoclonal antibody. CD4+ T cells from IL-17A$^{-/-}$ mice served as negative controls to demonstrate specificity and to establish background IL-17A staining levels.

Fibroblast culture. Mouse NIH3T6 fibroblasts were obtained from ATCC. Fibroblast cultures were maintained in Dulbecco's modified Eagle's medium supplemented with 10% fetal calf serum (Gibco BRL), 1% vitamin solutions, and 2 m*M* L-glutamine. For the experiments, cultures were placed in fresh, serum-free medium containing 0.1% bovine serum albumin for 24 hours prior to the addition of cytokines.

Fibroblast stimulation by IL-17A. Cultured fibroblasts were stimulated for 24 hours with the indicated final concentrations of recombinant IL-17A or TGFβ1. The concentration of soluble collagen in cultured fibroblast supernatants was measured using a Sircol soluble collagen assay kit (Biocolor), which is a dye-binding method for the analysis of acid- and pepsin-soluble collagens. Cultured fibroblasts were used for quantitative RT-PCR analysis of TGFβ1 and connective tissue growth factor (CTGF).

Statistical analysis. A Mann-Whitney U test was used for determining the significance of differences in sample means, and a Bonferroni test was used for multiple comparisons.

RESULTS

Amelioration of bleomycin-induced skin fibrosis by loss of IL-17A, but not IFNγ or IL-4. IFNγ, IL-4, and IL-17A are frequently used representatives of Th1, Th2, and Th17 cytokines, respectively. To determine which T helper cytokines are critical for bleomycin-induced skin fibrosis, we assessed the results of daily intradermal administration of bleomycin in IFN$\gamma^{-/-}$, IL-4$^{-/-}$, IL-17A$^{-/-}$, and WT mice. Dermal thickness, defined as the distance between the top of the granular layer and the dermal–adipose layer junction, was determined in 5 random grids on 3 different sections from each mouse (Figures 1A and B).

IL-17A deficiency caused a significant reduction in the mean dermal thickness, as evaluated by hematoxylin and eosin staining or Masson's trichrome staining. In contrast, the loss of IFNγ or IL-4 did not affect dermal thickness. The size of fibrotic areas, as evaluated by van Gieson's staining, was consistent with the findings for dermal thickness (Figure 1C). Likewise, the frequency of α-SMA–positive myofibroblasts and the local skin collagen content, which were evaluated in 3 different sections from each mouse, were significantly reduced in IL-17A–deficient mice (Figure 1C). The loss of IFNγ or IL-4 did not significantly affect the size of fibrotic areas, the frequency of myofibroblasts, or the skin collagen content. Thus, loss of IL-17A, but not IFNγ or IL-4, ameliorated skin fibrosis induced by daily intradermal bleomycin treatment.

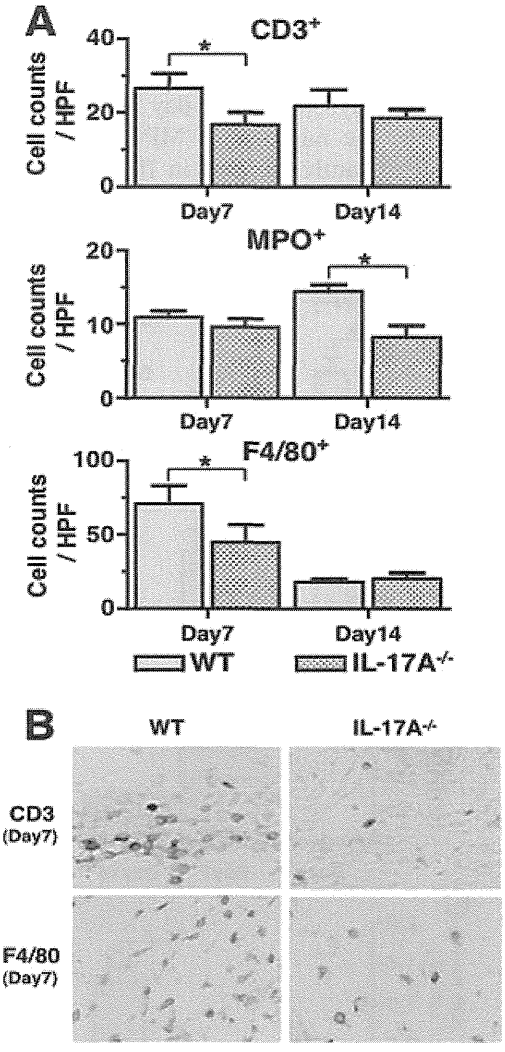

Figure 2. Inflammatory cell infiltration in the skin of IL-17A$^{-/-}$ mice and WT mice during intradermal bleomycin treatment. **A,** Numbers of CD3+ cells, myeloperoxidase (MPO)–positive neutrophils, and F4/80+ macrophages on day 7 and day 14. Bars show the mean ± SEM (n = 10 mice in each group). * = $P < 0.05$. **B,** Representative images showing CD3 and F4/80 staining in tissue sections from IL-17A$^{-/-}$ mice and WT mice. Original magnification × 400. See Figure 1 for other definitions.

Skin inflammation induced by daily intradermal bleomycin injections. Because we observed that only IL-17A loss affected skin fibrosis, subsequent experiments were performed solely in IL-17A$^{-/-}$ mice. The numbers of CD3+ T cells, MPO-positive neutrophils, and F4/80-positive macrophages were assessed in 5 random grids on 3 different sections of bleomycin-injected skin tissue specimens under 400× magnifica-

tion. When compared with skin tissue from WT mice, skin tissue from IL-17A$^{-/-}$ mice exhibited significantly reduced numbers of CD3+ T cells and F4/80-positive macrophages on day 7 but not on day 14 (Figures 2A and B). Conversely, the numbers of MPO-positive neutrophils were significantly reduced in IL-17A$^{-/-}$ mice on day 14 relative to WT controls (Figure 2A); the numbers of MPO-positive neutrophils in the 2 groups were not significantly different on day 7. Thus, inflammatory cell infiltration was generally modest in IL-17A$^{-/-}$ mice and was associated with reduced skin fibrosis.

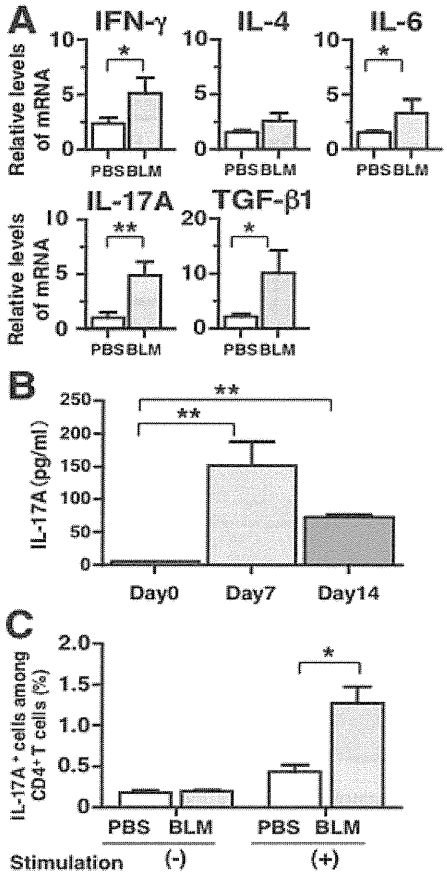

Figure 3. IL-17A expression in splenocytes and lesional skin from bleomycin-treated WT mice. **A,** Expression of IFNγ, IL-4, IL-6, IL-17A, and transforming growth factor β1 (TGFβ1) mRNA in CD4+ T cells isolated from the spleens of WT mice treated with bleomycin or PBS, as measured by quantitative reverse transcriptase–polymerase chain reaction on day 7. **B,** Concentrations of IL-17A in supernatants of skin homogenates, as measured by enzyme-linked immunosorbent assay. The total protein concentration in supernatants was equalized in each sample. **C,** Frequency of T cells that have potential to produce IL-17A. Splenocytes were harvested from WT mice that had been treated with bleomycin for 7 days. Purified CD4+ T cells were cultured in 96-well flat-bottomed plates precoated with anti-CD3 antibody plus anti-CD28 for 48 hours at 37°C. Cultured T cells were used for flow cytometric analysis of intracellular IL-17A. Each specimen was stimulated in triplicate wells. Bars show the mean ± SEM (n = 5 mice in each group). * = $P < 0.05$; ** = $P < 0.01$. See Figure 1 for other definitions.

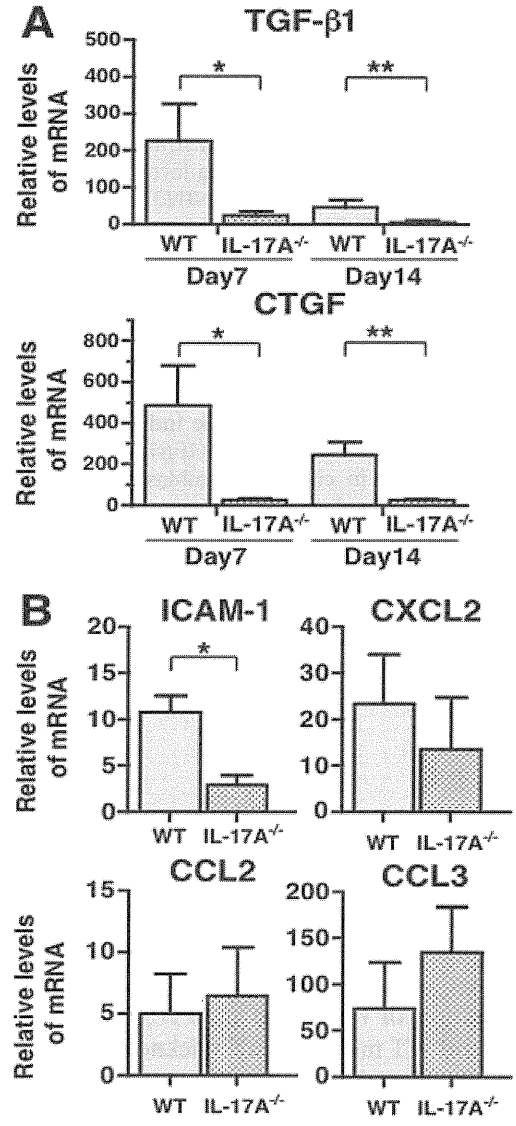

Figure 4. Messenger RNA levels of fibrogenic factors in IL-17A$^{-/-}$ mice. **A,** Expression of transforming growth factor β1 (TGFβ1) and connective tissue growth factor (CTGF) mRNA in bleomycin-treated WT mice and IL-17A$^{-/-}$ mice on days 7 and 14, as determined by quantitative reverse transcriptase–polymerase chain reaction (RT-PCR). **B,** Expression of intracellular adhesion molecule 1 (ICAM-1), CXCL2, CCL2, and CCL3 mRNA in bleomycin-treated WT and IL-17A$^{-/-}$ mice, as determined by quantitative RT-PCR on day 7. Bars show the mean ± SEM (n = 5 mice in each group). * = $P < 0.05$; ** = $P < 0.01$. See Figure 1 for other definitions.

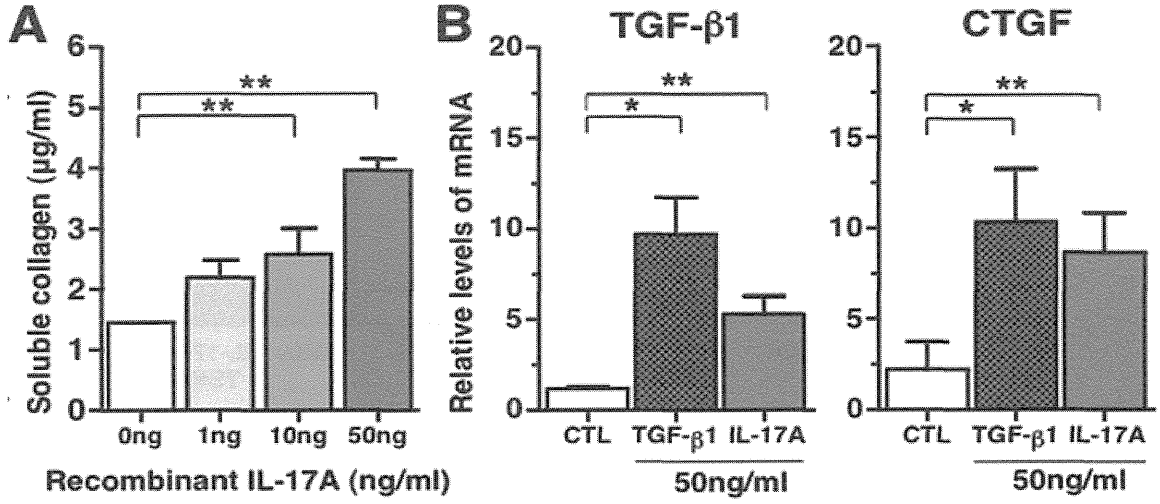

Figure 5. Effect of the addition of recombinant interleukin-17A (IL-17A) to a skin fibroblast cell line. **A,** IL-17A–induced dose-dependent increase in soluble collagen production, as determined using a Sircol soluble collagen assay kit. **B,** IL-17A–induced increase in transforming growth factor β1 (TGFβ1) and connective tissue growth factor (CTGF) mRNA expression. For comparison, recombinant TGFβ1 was also added to some cultures. Bars show the mean ± SEM results of 4 experiments. * = $P < 0.05$; ** = $P < 0.01$. CTL = control.

Effect of bleomycin on T cell cytokines. Next, we assessed mRNA levels of cytokines in CD4+ T cells isolated from the spleens of WT mice that received intradermal bleomycin injections. Overall, bleomycin treatment nonspecifically increased the expression of several cytokines, including IFNγ, IL-6, IL-17A, and TGFβ1 (Figure 3A). The induction of IL-17A was particularly prominent, with an ~5-fold increase compared with PBS-treated mice. For this reason, the concentration of IL-17A in skin lysates was measured by ELISA before and during bleomycin treatment. Interestingly, bleomycin injections significantly increased the local IL-17A concentration, with a peak on day 7 (Figure 3B).

We also evaluated whether bleomycin could induce Th17 cell differentiation. Initially, we examined whether bleomycin itself can directly affect in vitro Th17 cell differentiation, by culturing splenic T cells from WT mice in Th17 cell–inducing culture conditions. Although significant numbers of Th17 cells were induced during the in vitro Th17 cell differentiation assay (mean ± SEM 13.9 ± 3.4%), the frequency of Th17 cells was not significantly changed by the addition of bleomycin (10.5 ± 3.3%) (results not shown).

Next, we investigated whether daily intradermal bleomycin injections can induce Th17 cell induction in vivo. Bleomycin treatment significantly increased the frequency of T cells that have potential to produce IL-17A, although the population was small (Figure 3C). Thus, daily bleomycin injections can induce expression of cytokines, including IL-17A, in vivo. These findings indicated that bleomycin does not directly affect Th17 cell differentiation, but that daily bleomycin injections may indirectly enhance IL-17 production in the skin and splenic T cells.

Association of IL-17A loss with decreased mRNA expression of profibrogenic growth factors and intercellular adhesion molecule 1 (ICAM-1) in the skin. Fibrosis is influenced by a variety of cytokines and chemokines. We assessed whether IL-17A deficiency affects the expression of TGFβ and CTGF, 2 well-known fibrogenic growth factors, in the skin of mice receiving daily bleomycin injections. We observed that mRNA levels of both TGFβ and CTGF were markedly reduced on both day 7 and day 14 in mice deficient for IL-17A (Figure 4A). We also examined adhesion molecules and chemokines and observed that mRNA levels of ICAM-1 were significantly lower in IL-17A$^{-/-}$ mice than in WT controls on day 7 (Figure 4B). Messenger RNA levels of CXCL2, CCL2, and CCL3 were not significantly different between IL-17A$^{-/-}$ mice and WT mice on day 7. Thus, the local expression of TGFβ, CTGF, and ICAM-1 was decreased in the skin of bleomycin-treated IL-17A$^{-/-}$ mice.

Effect of recombinant IL-17A on collagen production from fibroblasts. To confirm the direct effect of IL-17A on fibrosis, we cultured a mouse fibroblast cell line with or without recombinant IL-17A. Consistent

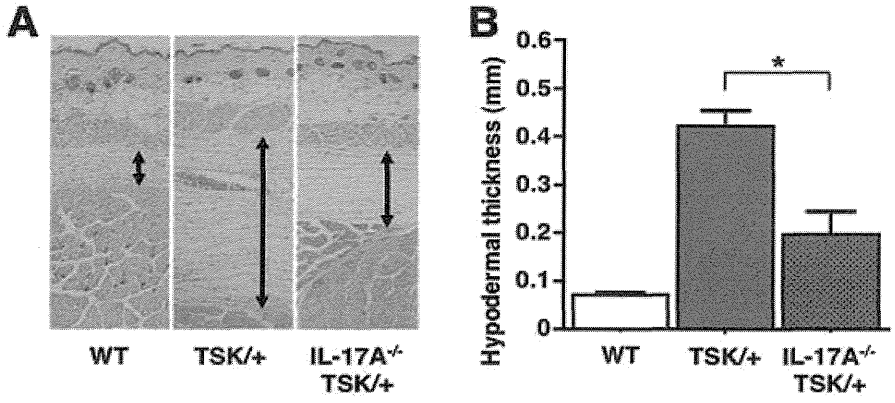

Figure 6. Atttenuation of hypodermal thickness by IL-17A deficiency in TSK/+ mice. **A,** Representative hematoxylin and eosin–stained skin tissue sections from WT, TSK/+, and IL-17A$^{-/-}$ TSK/+ mice. **Arrows** indicate the thickness of the hypodermis beneath the panniculus carnosus. Original magnification × 40. **B,** Hypodermal thickness in WT mice, TSK/+ mice, and IL-17A$^{-/-}$ TSK/+ mice. Bars show the mean ± SEM (n = 5 mice in each group). * = $P < 0.05$. See Figure 1 for definitions.

with our in vivo data, the addition of IL-17A resulted in a dose-dependent increase in the production of soluble collagen (Figure 5A). Furthermore, TGFβ and CTGF mRNA expression was increased in cultured fibroblasts following the addition of IL-17A (Figure 5B). These findings indicate that IL-17A can stimulate collagen synthesis from skin fibroblasts, directly and/or indirectly, via fibroblast production of cytokines such as TGFβ and CTGF.

Reduced skin thickness in IL-17A–deficient TSK mice. We further analyzed the fibrotic potential of IL-17A in the TSK/+ mouse model, a genetic mouse model of SSc that resembles the later stages of SSc and is characterized by endogenous activation of fibroblasts without inflammatory infiltration (20,27). In TSK/+ mice, skin fibrosis is established by age 10 weeks and is attributable to marked hypodermal thickness. Hypodermal thickness, which was defined as the thickness of a subcutaneous loose connective tissue layer (i.e., the hypodermis or superficial fascia) beneath the panniculus carnosus, was measured in 5 grids on 3 different sections of each mouse. Hypodermal thickness was significantly reduced in IL-17A$^{-/-}$ TSK/+ mice compared with control TSK/+ mice (Figure 6).

DISCUSSION

By using cytokine-deficient mice, we determined that IL-17A, but not IFNγ or IL-4, is necessary for maximal bleomycin-induced skin fibrosis. Among mice deficient for IFNγ, IL-4, or IL-17A, only IL-17A–deficient mice demonstrated reduced skin fibrosis following bleomycin treatment. Daily intradermal bleomycin injections triggered IL-17A production in the lesional skin. Additionally, IL-17A was critical for the induction of TGFβ and CTGF in fibrotic skin during bleomycin treatment. The addition of recombinant IL-17A to a skin fibroblast cell line increased the production of collagen, TGFβ, and CTGF. Furthermore, the loss of IL-17A also significantly reduced skin thickness in another model of SSc, TSK/+ mice, suggesting the critical roles of IL-17A in skin fibrosis.

To our knowledge, this study is the first to identify specific roles for IL-17A in the bleomycin-induced skin fibrosis model, via the use of transgenic mice or blocking antibodies. Recently, IL-17A has been implicated in the development of tissue fibrosis and SSc. For example, IL-17A was shown to be critically involved in the development of bleomycin-, silica-, or IL-1β–induced lung fibrosis (10,28,29), and serum IL-17A levels were increased in mice treated with daily intradermal bleomycin injections (30). Elevated serum IL-17A levels and augmented IL-17A expression in peripheral blood lymphocytes and lesional skin have also been reported in patients with SSc (11,12). Another study demonstrated that patients with SSc had markedly increased numbers of circulating Th17 cells (7,31). In addition, a crucial role for IL-17A in sclerodermatous chronic graft-versus-host disease has been reported (32). Our findings support these observations and extend them, by providing a potential and possibly important function for IL-17A in promoting skin fibrosis.

To clarify the mechanism behind IL-17A regula-

tion of fibrosis, we first determined whether bleomycin could induce IL-17A production. Splenic T cells from WT mice treated intradermally with bleomycin had augmented IFNγ, IL-6, IL-17A, and TGFβ1 mRNA expression; the increase in IL-17A expression was most striking. In addition, daily intradermal bleomycin injections markedly increased the IL-17A concentration in lesional skin, with a peak on day 7. These findings are similar to those of a recent study that showed elevated IL-17A expression in the bronchoalveolar lavage fluid and lung tissue of mice with bleomycin-induced lung fibrosis (10). In our study, daily bleomycin injections increased the potential source of Th17 cells in splenocytes. These findings suggest that the augmented IL-17A production induced by bleomycin treatment cooperated with other proinflammatory or profibrogenic cytokines to promote the development of skin fibrosis.

Although IL-17A has been shown to promote fibroblast proliferation, the direct effect of IL-17A on collagen synthesis in humans has not been reported (11). Therefore, IL-17A may be contributing to the development of skin fibrosis indirectly via induction of other molecules critical for fibrosis or inflammation. To examine this possibility, we examined mRNA expression of profibrogenic molecules in the bleomycin-induced fibrotic skin of IL-17A$^{-/-}$ mice, using real-time RT-PCR. The expression of TGFβ, CTGF, and ICAM-1 mRNA was dramatically reduced by the loss of IL-17A. Because TGFβ and CTGF are central players in the fibrotic process (1), induction of these cytokines by IL-17A is likely important for the development of skin fibrosis in vivo.

ICAM-1 is also considered to be important for skin fibrosis and/or skin inflammation in both bleomycin-induced skin fibrosis and in TSK/+ mice (30,33). Our results are consistent with those from a prior study that revealed roles for IL-17A in ICAM-1 induction in human endothelial cells (11). Furthermore, human IL-17A has been shown to induce cytokines such as IL-6, IL-8, and granulocyte colony-stimulating factor from fibroblasts (34). Our data agree with these previous findings and indicate that IL-17A may be contributing indirectly to bleomycin-induced skin fibrosis via induction of adhesion molecules and various profibrogenic and proinflammatory cytokines.

Consistent with these in vivo data, we observed that recombinant IL-17A enhanced the expression of both TGFβ and CTGF in a cultured mouse skin fibroblast cell line. Furthermore, the addition of IL-17A increased collagen synthesis in these fibroblasts. In a recent study, mRNA levels of Colα2(I) and TGFβ were shown to be increased in cultured fibroblasts derived from mouse skin (30). Although our current results are similar to those of the previous study, we also detected increased CTGF expression in cultured fibroblasts following the addition of IL-17A. However, it is unclear whether the augmented collagen synthesis was directly caused by IL-17A. Another previous study showed that intratracheal administration of IL-17A induced lung fibrosis that was TGFβ dependent (10). Furthermore, an analysis of T helper cell subsets demonstrated that Th17 cells were the main producers of TGFβ1 both in vivo and in vitro (35). Therefore, our results for fibroblasts may also be reflecting the effects of increased TGFβ production. Further studies will be needed to determine whether IL-17A is directly affecting CTGF production by fibroblasts, and whether CTGF is contributing to IL-17A–induced collagen synthesis.

IL-17A and Th17 cells have been considered to be critical mediators of various autoimmune diseases and inflammatory bowel or skin diseases, in addition to their roles in host defense (8,9). However, fibrotic changes are uncommon in these disorders. This may be due to different functions and/or expression of IL-17A or Th17 cells that is dependent on each disease, organ, phase, and environment (expression of other cytokines). In fact, recent studies showed significant plasticity of Th17 cells and suggested the possibility that the pathogenetic function of these cells may be mediated through a Th17-to-Th1 phenotype (IFNγ producer) transition in other autoimmune conditions such as autoimmune colitis and diabetes (36,37). In contrast, Th17 cells require TGFβ for sustained expression of IL-17A (37). Therefore, in a TGFβ-rich environment such as fibrotic disorders (including SSc), Th17-to-Th1 conversions may be infrequent compared with the conversions that occur in other autoimmune or inflammatory disorders. Furthermore, TGFβ is highly expressed by Th17 cells and acts in an autocrine manner to maintain Th17 cells (35). Therefore, the function of IL-17A and Th17 may be different depending on the profile of cytokines and Th cell subsets that contribute to the development of each disease.

Recently, a list of criteria to use in selecting the most promising molecular targets for SSc trials was proposed (38). According to those criteria, the antifibrotic effects of specific molecules should be confirmed in at least 2 complementary animal models of SSc. Although in the current study we mainly analyzed the roles of IL-17A in a model of bleomycin-induced SSc, similar findings were also observed in TSK/+ mice. Bleomycin-induced skin fibrosis is characterized by dense inflammatory cell infiltration in lesional skin.

Inflammatory cells have been considered to contribute to the development of skin fibrosis by stimulating profibrogenic cytokine production from fibroblasts. In contrast, TSK/+ mice are characterized by the absence of inflammation and by endogenous activation of fibroblasts. Thereby, the bleomycin-induced model and the TSK/+ mouse model mimic the early progressive stage and the late stage of SSc, respectively (27). Thus, our data indicate that IL-17A has fibrotic effects in 2 mouse models of SSc with different pathologic mechanisms.

We believe that further studies that include the administration of blocking antibody will be needed to clarify the roles of IL-17A in the development of SSc. Nonetheless, our findings suggest that inhibition of IL-17A represents a promising therapeutic target for antagonizing fibrotic skin disorders such as SSc. Because anti-human monoclonal antibodies against IL-17A or IL-17 receptor have been used for clinical trials in other autoimmune and inflammatory disorders (39–41), this strategy could be rapidly advanced into clinical trial testing in patients with SSc.

ACKNOWLEDGMENTS

We thank Dr. W. Ishida, for technical advice and Ms M. Matsubara and Y. Yamada for technical assistance.

AUTHOR CONTRIBUTIONS

All authors were involved in drafting the article or revising it critically for important intellectual content, and all authors approved the final version to be published. Dr. Hasegawa had full access to all of the data in the study and takes responsibility for the integrity of the data and the accuracy of the data analysis.

Study conception and design. Okamoto, Hasegawa, Fujimoto.

Acquisition of data. Okamoto.

Analysis and interpretation of data. Okamoto, Hasegawa, Matsushita, Hamaguchi, Huu, Iwakura, Fujimoto, Takehara.

REFERENCES

1. Varga J, Abraham D. Systemic sclerosis: a prototypic multisystem fibrotic disorder. J Clin Invest 2007;117:557–67.
2. Gabrielli A, Avvedimento EV, Krieg T. Scleroderma. N Engl J Med 2009;360:1989–2003.
3. Wynn TA. Fibrotic disease and the T_H1/T_H2 paradigm. Nat Rev Immunol 2004;4:583–94.
4. Boin F, De Fanis U, Bartlett SJ, Wigley FM, Rosen A, Casolaro V. T cell polarization identifies distinct clinical phenotypes in scleroderma lung disease. Arthritis Rheum 2008;58:1165–74.
5. Abraham DJ, Varga J. Scleroderma: from cell and molecular mechanisms to disease models. Trends Immunol 2005;26:587–95.
6. Sakkas LI, Platsoucas CD. Is systemic sclerosis an antigen-driven T cell disease? [review]. Arthritis Rheum 2004;50:1721–33.
7. Radstake TR, van Bon L, Broen J, Hussiani A, Hesselstrand R, Wuttge DM, et al. The pronounced Th17 profile in systemic sclerosis (SSc) together with intracellular expression of TGFβ and IFNγ distinguishes SSc phenotypes. PLoS One 2009;4:e5903.
8. Korn T, Bettelli E, Oukka M, Kuchroo VK. IL-17 and Th17 cells. Annu Rev Immunol 2009;27:485–517.
9. Iwakura Y, Ishigame H, Saijo S, Nakae S. Functional specialization of interleukin-17 family members. Immunity 2011;34:149–62.
10. Wilson MS, Madala SK, Ramalingam TR, Gochuico BR, Rosas IO, Cheever AW, et al. Bleomycin and IL-1β-mediated pulmonary fibrosis is IL-17A dependent. J Exp Med 2010;207:535–52.
11. Kurasawa K, Hirose K, Sano H, Endo H, Shinkai H, Nawata Y, et al. Increased interleukin-17 production in patients with systemic sclerosis. Arthritis Rheum 2000;43:2455–63.
12. Murata M, Fujimoto M, Matsushita T, Hamaguchi Y, Hasegawa M, Takehara K, et al. Clinical association of serum interleukin-17 levels in systemic sclerosis: is systemic sclerosis a Th17 disease? J Dermatol Sci 2008;50:240–2.
13. Gourh P, Arnett FC, Assassi S, Tan FK, Huang M, Diekman L, et al. Plasma cytokine profiles in systemic sclerosis: associations with autoantibody subsets and clinical manifestations. Arthritis Res Ther 2009;11:R147.
14. Yamamoto T, Takagawa S, Katayama I, Yamazaki K, Hamazaki Y, Shinkai H, et al. Animal model of sclerotic skin. I: Local injections of bleomycin induce sclerotic skin mimicking scleroderma. J Invest Dermatol 1999;112:456–62.
15. Yamamoto T, Takagawa S, Kuroda M, Nishioka K. Effect of interferon-γ on experimental scleroderma induced by bleomycin. Arch Dermatol Res 2000;292:362–5.
16. Chen ES, Greenlee BM, Wills-Karp M, Moller DR. Attenuation of lung inflammation and fibrosis in interferon-γ-deficient mice after intratracheal bleomycin. Am J Respir Cell Mol Biol 2001;24:545–55.
17. Ong C, Wong C, Roberts CR, Teh HS, Jirik FR. Anti-IL-4 treatment prevents dermal collagen deposition in the tight-skin mouse model of scleroderma. Eur J Immunol 1998;28:2619–29.
18. McGaha T, Saito S, Phelps RG, Gordon R, Noben-Trauth N, Paul WE, et al. Lack of skin fibrosis in tight skin (TSK) mice with targeted mutation in the interleukin-4R α and transforming growth factor-β genes. J Invest Dermatol 2001;116:136–43.
19. Izbicki G, Breuer R. IL-4 is not a key profibrotic cytokine in bleomycin-induced lung fibrosis model. J Immunol 2003;171:2767–8.
20. Green MC, Sweet HO, Bunker LE. Tight-skin, a new mutation of the mouse causing excessive growth of connective tissue and skeleton. Am J Pathol 1976;82:493–512.
21. Kopf M, Le Gros G, Bachmann M, Lamers MC, Bluethmann H, Kohler G. Disruption of the murine IL-4 gene blocks Th2 cytokine responses. Nature 1993;362:245–8.
22. Nakae S, Komiyama Y, Nambu A, Sudo K, Iwase M, Homma I, et al. Antigen-specific T cell sensitization is impaired in IL-17-deficient mice, causing suppression of allergic cellular and humoral responses. Immunity 2002;17:375–87.
23. Tagawa Y, Sekikawa K, Iwakura Y. Suppression of concanavalin A-induced hepatitis in IFN$\gamma^{-/-}$ mice, but not in TNF-$\alpha^{-/-}$ mice: role for IFNγ in activating apoptosis of hepatocytes. J Immunol 1997;159:1418–28.
24. Lopez-De Leon A, Rojkind M. A simple micromethod for collagen and total protein determination in formalin-fixed paraffin-embedded sections. J Histochem Cytochem 1985;33:737–43.
25. Meijerink J, Mandigers C, van de Locht L, Tonnissen E, Goodsaid F, Raemaekers J. A novel method to compensate for different amplification efficiencies between patient DNA samples in quantitative real-time PCR. J Mol Diagn 2001;3:55–61.
26. Mori R, Kondo T, Nishie T, Ohshima T, Asano M. Impairment of skin wound healing in β-1,4-galactosyltransferase-deficient mice with reduced leukocyte recruitment. Am J Pathol 2004;164:1303–14.
27. Akhmetshina A, Venalis P, Dees C, Busch N, Zwerina J, Schett G, et al. Treatment with imatinib prevents fibrosis in different

preclinical models of systemic sclerosis and induces regression of established fibrosis. Arthritis Rheum 2009;60:219–24.
28. Gasse P, Riteau N, Vacher R, Michel ML, Fautrel A, di Padova F, et al. IL-1 and IL-23 mediate early IL-17A production in pulmonary inflammation leading to late fibrosis. PLoS One 2011;6: e23185.
29. Mi S, Li Z, Yang HZ, Liu H, Wang JP, Ma YG, et al. Blocking IL-17A promotes the resolution of pulmonary inflammation and fibrosis via TGF-β1-dependent and -independent mechanisms. J Immunol 2011;187:3003–14.
30. Yoshizaki A, Yanaba K, Iwata Y, Komura K, Ogawa A, Akiyama Y, et al. Cell adhesion molecules regulate fibrotic process via Th1/Th2/Th17 cell balance in a bleomycin-induced scleroderma model. J Immunol 2010;185:2502–15.
31. Truchetet ME, Brembilla NC, Montanari E, Allanore Y, Chizzolini C. Increased frequency of circulating Th22 in addition to Th17 and Th2 lymphocytes in systemic sclerosis: association with interstitial lung disease. Arthritis Res Ther 2011;13:R166.
32. Hill GR, Olver SD, Kuns RD, Varelias A, Raffelt NC, Don AL, et al. Stem cell mobilization with G-CSF induces type 17 differentiation and promotes scleroderma. Blood 2010;116:819–28.
33. Matsushita Y, Hasegawa M, Matsushita T, Fujimoto M, Horikawa M, Fujita T, et al. Intercellular adhesion molecule-1 deficiency attenuates the development of skin fibrosis in tight-skin mice. J Immunol 2007;179:698–707.
34. Fossiez F, Djossou O, Chomarat P, Flores-Romo L, Ait-Yahia S, Maat C, et al. T cell interleukin-17 induces stromal cells to produce proinflammatory and hematopoietic cytokines. J Exp Med 1996;183:2593–603.
35. Gutcher I, Donkor MK, Ma Q, Rudensky AY, Flavell RA, Li MO. Autocrine transforming growth factor-β1 promotes in vivo Th17 cell differentiation. Immunity 2011;34:396–408.
36. Wei G, Wei L, Zhu J, Zang C, Hu-Li J, Yao Z, et al. Global mapping of H3K4me3 and H3K27me3 reveals specificity and plasticity in lineage fate determination of differentiating $CD4^+$ T cells. Immunity 2009;30:155–67.
37. Lee YK, Turner H, Maynard CL, Oliver JR, Chen D, Elson CO, et al. Late developmental plasticity in the T helper 17 lineage. Immunity 2009;30:92–107.
38. Distler JH, Distler O. Criteria to select molecular targets for anti-fibrotic therapy. Rheumatology (Oxford) 2008;47 Suppl 5:v12–3.
39. Genovese MC, Van den Bosch F, Roberson SA, Bojin S, Biagini IM, Ryan P, et al. LY2439821, a humanized anti–interleukin-17 monoclonal antibody, in the treatment of patients with rheumatoid arthritis: a phase I randomized, double-blind, placebo-controlled, proof-of-concept study. Arthritis Rheum 2010;62:929–39.
40. Papp KA, Leonardi C, Menter A, Ortonne JP, Krueger JG, Kricorian G, et al. Brodalumab, an anti-interleukin-17-receptor antibody for psoriasis. N Engl J Med 2012;366:1181–9.
41. Leonardi C, Matheson R, Zachariae C, Cameron G, Li L, Edson-Heredia E, et al. Anti-interleukin-17 monoclonal antibody ixekizumab in chronic plaque psoriasis. N Engl J Med 2012;366: 1190–9.

DOI:10.1111/j.1600-0625.2011.01419.x
www.blackwellpublishing.com/EXD

Original Article

Local injection of latency-associated peptide, a linker propeptide specific for active form of transforming growth factor-beta1, inhibits dermal sclerosis in bleomycin-induced murine scleroderma

Taeko Nakamura-Wakatsuki, Noritaka Oyama and Toshiyuki Yamamoto

Department of Dermatology, Fukushima Medical University, Fukushima, Japan
Correspondence: Taeko Nakamura-Wakatsuki, Department of Dermatology, Fukushima Medical University, Hikarigaoka 1, Fukushima 960-1295, Japan, Tel.: +81-24-547-1309, Fax: +81-24-548-5412, e-mail: tn-0203@fmu.ac.jp

Abstract: Transforming growth factor-β1 (TGF-β1) has been thought to play a key role in the pathogenesis of scleroderma; however, therapeutic approaches targeting TGF-β1 and/or related molecules have provided inconsistent results. In this study, we demonstrate the antifibrotic effects of local administration of latency-associated peptide (LAP), a linker propeptide that specifically converts the active form of TGF-β1 to the inactive from, in the bleomycin (BLM)-induced scleroderma mouse model. Histologically, co-injection of BLM and LAP into the dorsal skin prevented proinflammatory and later sclerotic responses, features seen in mice injected with BLM alone or together with PBS as control. In addition, the skin sites co-injected with BLM and LAP showed a marked decrease in mast cell infiltration. Isoform-specific ELISA and real-time RT-PCR revealed transient decreases in connective tissue growth factor and collagen α1(I) mRNA expression 2 weeks after the co-injection, preceded by a decrease in active TGF-β1 protein production. In contrast, the baseline expression of TGF-β1 mRNA remained unchanged. By contrast, after induction of scleroderma by BLM, the inhibitory effects of LAP did not occur, suggesting time course–dependent TGF-β1 regulation. Our data may have novel therapeutic implications regarding *in vivo* TGF-β1 inactivation in human scleroderma, and the post-transcriptional interrelationship between major fibrogenic cytokines in the autoimmune aspects of the disease.

Key words: bleomycin – latency-associated peptide – mouse model – scleroderma – transforming growth factor-β

Accepted for publication 15 November 2011

Introduction

Systemic sclerosis (SSc) is an autoimmune-based, multisystem connective tissue disorder of unknown aetiology, characterized by fibrosis and microvascular injury in the affected organs (1). The disease affects all organ systems, particularly skin, blood vessels, lungs, kidneys, gastrointestinal tract and heart, thus resulting in high morbidity and mortality. The pathological events in scleroderma may vary considerably; they include impaired communication between endothelial cells, epithelial cells, fibroblasts, activation of local lymphocytes and mast cells, and persistent inflammation via dysregulation of cytokines, chemokines and growth factors (2). Serum autoantibody profiles characteristic of the disease may potentially reflect particular clinical states and symptoms (3) and also affect inflammatory and sclerotic activities of the disease. However, the immunopathogenic nature of scleroderma has yet to be fully elucidated.

One putative candidate for the underlying molecular pathology in scleroderma is a multifactorial cytokine, transforming growth factor-β (TGF-β). The rationale for the role of TGF-β is based on a series of studies demonstrating fibrogenic and sclerotic properties of TGF-β1 and related molecules (e.g. the downstream intracellular effector of TGF-β, Smads), in human scleroderma and animal models of the disease; for example, we have previously showed the therapeutic effects of anti-TGF-β1 neutralizing antibody in the bleomycin (BLM)-induced scleroderma mouse model (4). The genetic ablation of Smad3 (Smad 3-null mice) reduced BLM-induced fibrosis and collagen synthesis (5).

Transforming growth factor-beta1 belongs to the TGF-β family that is ubiquitously expressed in most tissues and exerts a wide variety of biological actions on cell growth and differentiation, apoptosis, cell migration, adhesion and deposition of extracellular matrix (ECM) proteins. There are five distinct TGF-β isoforms, of which three (TGF-β1, 2 and 3) are present in mammals. The basic structure of the three TGF-βs is highly conserved among species, but their biological activities may be different. TGF-β1 forms a pro-precursor molecule, consisting of the N-terminal signal peptide, a pro-region latency-associated peptide (LAP) and the C-terminal mature peptide. Post-translational processing yields the small latent complex, a non-covalent association between two LAPs and two mature homodimerized peptides. Finally, the latent complex can be converted to the active form by acidic (pH < 3.5) or alkaline conditions (pH > 12.5), heat treatment (>80°C, 10 min), certain glycosidases and the protease plasmin, thrombospondin-1, reactive oxygen species and integrin $\alpha v\beta 5$ (6). The activation step is indispensable for the biological activity of TGF-β1 upon binding to its cell surface receptors. The potential importance of biological TGF-β1 conversion is supported by evidence that overexpression of the latent form of TGF-β1 can attenuate the renal inflammation and fibrosis in the mouse model of obstructive kidney disease (7,8). A clinical trial for *in vivo* use of human TGF-β1 neutralizing therapy in SSc patients produced no evidence of efficacy (9). However, the TGF-β1 targeting approach warrants further evaluation considering the cascade-specific efficacy of TGF-β1 in the treatment of scleroderma. Furthermore, injection of LAP recombinant protein prevented liver fibrosis (10), and human recombinant LAP prevented skin and lung fibrosis in sclerodermatous graft-versus-host disease (Scl-GvHD) mice (11). In this study, we examined the potential

benefit of local LAP administration on mouse scleroderma induced by BLM.

Materials and methods

Mice and reagents

Specific pathogen-free CH3/HeJ female mice (6 week old) were purchased from Clea Japan (Tokyo, Japan) and housed in a controlled environment (21–24°C, 60% humidity, 12-h light/dark cycle). BLM and recombinant human LAP were from Nippon Kayaku Co. Ltd. (Tokyo, Japan) and R&D Systems (Minneapolis, MN, USA), respectively. All experimental procedures in this study were approved by the Animal Care Committee of Fukushima Medical University.

Induction of BLM-induced scleroderma in mice and local injection of LAP

The scleroderma mouse model was established according to our previous study (12). Briefly, BLM was dissolved in phosphate-buffered saline (PBS) at a final concentration of 250 μg/ml. After filter sterilization, 100 μl of BLM was intradermally injected into the shaved back of the mice once daily for 5 days/week for 4 weeks.

For experiments using an 'ongoing' LAP treatment, 100 μl of BLM and either 50 or 500 ng of recombinant LAP (final concentrations of 50 or 500 ng/ml in PBS, respectively) were co-injected intradermally for consecutive 4 weeks. The same volumes of BLM and PBS were used as a control combination.

In 'post-onset' experiments, after 4-weeks' injection of BLM alone, 50 ng of LAP was injected subsequently into the BLM-treated skin sites for another 2 weeks. The LAP doses were optimized on the basis of sequential pilot experiments. Each mouse was randomly assigned to one of three groups: LAP (50 ng/ml), LAP (500 ng/ml) and control PBS (n = 4–7 in each group).

Histopathological analysis

The injected skin sites were punch-biopsied (6 mm) and cut into at least two pieces: one was used for paraffin-embedded sectioning and the other was stored immediately in liquid nitrogen for cryosectioning. For evaluation of skin sclerosis, the skin section was stained by the Elastica–Masson's method, and dermal thickness was then measured as collagen thickness computationally under equal magnification (×100) using a light microscope. Infiltrating mast cells were characterized by toluidine blue staining, counted in at least three distinct fields under a light microscope at a magnification of ×400 and then expressed as mean cell numbers ± SD.

ELISA

To determine the amounts of active and total (active/latent) TGF-β1 protein in the injected skin, the block of biopsied skin was homogennized on ice and centrifuged (×12 000) for 10 min at 4°C. Equal volumes of the supernatants obtained were initially treated with 1N acetic acid to convert the latent form of TGF-β1 to its active form and then subjected to commercially available ELISA specific for mouse TGF-β1 according to the manufacturer's instructions (R&D systems). Based on the previous procedure used (13), the spontaneously converted active form of TGF-β1 protein was similarly measured without acid pretreatment. The amounts of bulk protein were determined by the Bradford method and used to optimize the amounts of TGF-β1 protein in each sample (n = 5–6 in each).

Hydroxyproline contents

Collagen deposition and fibrosis were estimated by determining the total hydroxyproline content of the skin. The stored skins were dried for 20 h in a 110°C incubator. After drying the tissues, they were hydrolysed in 6N hydrochloric acid at 110°C for 24 h. After neutralizing with appropriate amounts of 6N sodium hydroxide, the hydrolysates were diluted with distilled water. The hydrolysates were mixed after adding 2 g of KCl and kept on ice for 15 min. The mixture was oxidized with 1.0 ml of 0.2 M chloramine-T solution and kept on ice for 120 min. The oxidation reaction was stopped by adding 2 ml of 3.6 M sodium thiosulfate in boiling water for 30 min. After cooling to room temperature, the product was mixed with 2.0 ml of toluene and centrifuged at 300–400 g for 5 min to separate the pyrrole reaction product. The final pyrrole reaction product contained in 2.0 ml of the toluene layer was mixed with 0.8 ml of Ehrlich's reagent and was measured against hydroxyproline standards at 650 and 562 nm. Hydroxyproline contents are given per 100 μl volume of the hydrolysate.

Real-time reverse transcriptase polymerase chain reaction

Total RNA was extracted from frozen skin tissue using ISOGEN® (NIPPON GENE, Tokyo, Japan) and was treated with DNase (TURBO DNase Kit; Applied Biosystems, Carlsbad, CA, USA), followed by reverse transcription to synthesize single-strand cDNA with random hexamers (High Capacity RNA-to-cDNA Kit; Applied Biosystems). Serial dilution of the cDNA obtained was cycle-amplified specifically with specific primer sets for GAPDH either with TGF-β1, connective tissue growth factor (CTGF) or collagen α1(I).

for TGF-β1 Sense: 5′-TTTCCGCTGCTACTGCAAGTC-3′
Antisense: 3′ AGGGCTGTCTGGAGTCCTCA-5′
for CTGF Sense: 5′-ACCCGAGTTACCAATGACAA-TACC-3′
Antisense: 3′-CCGCAGAACTTAGCCCTGTATG-5′
for collagen α1(I) Sense: 5′- CAGGGTATTGCTGGACA ACGTG-3′
Antisense: 3′- GGACCTTGTTTGCCAGGTTCA-5′
for GAPDH Sense: 5′-TGTGTCCGTCGTGGATCTGA-3′
Antisense: 3′-TTGCTGTTGAAGTCGCAGGAG-5′

All the primers were designed using the Perfect Real Time support system (Takara Bio, Shiga, Japan). The PCR mixture contained 2 μl (serially equating 0.2–200 ng/μl) of cDNA, 7 μl DNase, 10× PCR SYBR Green Master mix (Applied Biosystems) and oligonucleotide primer sets in a volume of 25 μl nuclease-free water. PCR was carried out under a logarithmic phase of amplification as follows: 95°C for 5 min, followed by 40 cycles of amplification; 95°C for 30 s, 58°C for 30 s and 72°C for 30 s using the ABI Step One system (Applied Biosystems). The transcription ratio for each expressed molecule against GAPDH was indicated.

Statistical analysis

All of the data were expressed as mean ± SD and analysed using Statview software version 5.0 (SAS Institute Inc., Cary, NC, USA). Differences between BLM-treated and BLM-untreated mice in the median value of each parameter were evaluated by an unpaired Mann–Whitney U-test. A P-value < 0.05 was considered as statistically significant.

Results

Local LAP treatment rescues BLM-induced scleroderma in mice

We have previously established a scleroderma mouse model produced by local injection of BLM (12). The model reproduces the

overall pathophysiology of human scleroderma, encompassing skin and lung fibrosis and serum autoantibodies characteristic of the disease. Using this reliable model, we examined the antifibrotic effects of LAP, a linker propeptide that specifically neutralizes the active form of TGF-β1, on BLM-induced dermal sclerosis. Initially, we confirmed that injection of BLM into the dorsal skin of C3H/HeJ mice over a 4-week period can induce skin sclerosis. The histology of the injected skin sites revealed thickening of dermal collagen bundles and increased deposition of collagen fibres, as assessed by Elastica–Masson's staining, a pathology consistent with human scleroderma.

We next addressed whether active TGF-β1 affects the establishment of scleroderma in BLM-treated mice *in vivo*, and if so, whether local TGF-β1 inactivation can rescue the sclerotic change. In experiments of the 'ongoing' type, BLM and LAP were co-injected daily into the mouse's dorsal skin for 4 weeks. Histology of the co-injected skin sites showed decreases in thickness of the local collagen fibres (Fig. 1a–h). Dermal thickness of the LAP-treated skin was significantly reduced compared with skin treated with PBS as a control [LAP (50 ng): 204.0 ± 19.70 μm vs PBS: 269.4 ± 48.43 μm, $P = 0.025$; LAP (500 ng): 176.5 ± 28.20 μm vs PBS: 269.4 ± 48.43 μm, $P = 0.014$] (Fig. 1i). However, the inhibitory effects of LAP were statistically identical at the two doses used, indicating lack of dose dependency.

By contrast, in the 'post-onset' experiments, BLM pretreatment prior to a 4-week period of co-injection with LAP failed to reverse any of the skin sclerotic features (data were not shown), suggesting time-dependent regulation of the TGF-β1 system in BLM-induced scleroderma.

LAP injection reduces mast cell infiltration in BLM-induced scleroderma

After 4 weeks of injection of BLM, intradermal infiltration of mast cells into the injected skin sites was increased significantly, as assessed by toluidine blue staining (Fig. 2a–c). The 4-week period of co-injection of BLM with LAP decreased the BLM-induced infiltration of mast cells (Fig. 2d), suggesting a TGF-β inactivation-specific action on BLM-induced mast cell migration. However, the LAP doses did not significantly affect numbers of infiltrating mast cells [LAP (50 ng): 9.25 ± 1.52/HPF vs PBS: 13.60 ± 3.09/HPF, $P = 0.041$; LAP (500 ng): 8.66 ± 3.66/HPF vs PBS: 13.60 ± 3.09/HPF, $P = 0.038$].

LAP injection reduces hydroxyproline content in the skin

Bulk collagen content was measured in the skin sites co-injected with BLM and LAP for 2 weeks. The levels of hydroxyproline in

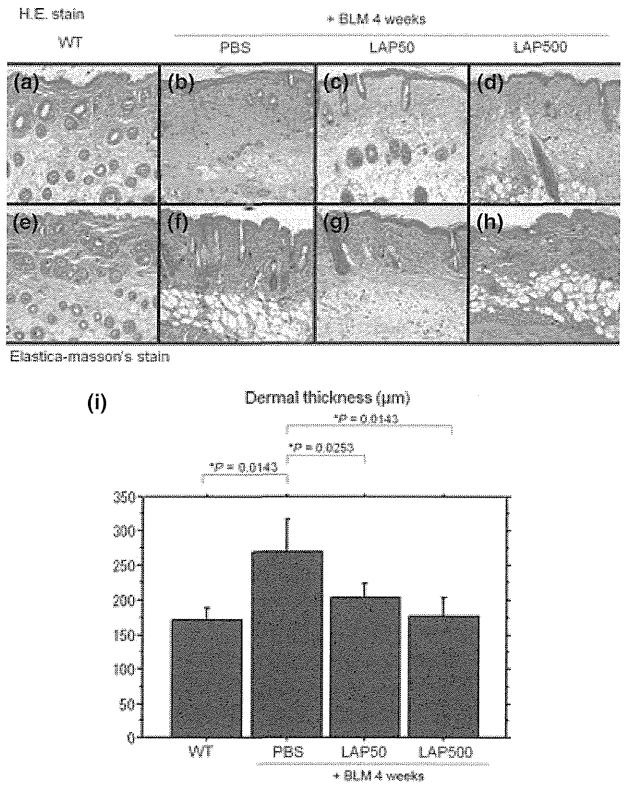

Figure 1. Histopathological evaluation of effects of co-injection of bleomycin (BLM) and latency-associated peptide (LAP) for 4 weeks. (a–d; Haematoxylin and eosin stain). (a) Epidermis and dermis of wild-type C3H/HeJ mice without any treatment. (b) Mice were treated by co-injection of BLM (500 μg/ml) and PBS as a control for 4 weeks. Marked dermal sclerosis with increased skin thickness and homogenous collagen bundles. (c) Mice in the LAP group were co-injected with BLM (500 μg/ml) and LAP (50 ng/ml) for 4 weeks. Dermal sclerosis was reduced compared with the PBS-treated control group. (d) Another LAP-treated group was injected with BLM (500 μg/ml) and LAP (500 ng/ml) for 4 weeks. However, there was no statistically significant dose dependence of LAP-induced inhibition. (e–h; Elastica–masson's stain). LAP-induced reduction in collagen bundle and dermal thickness is shown more clearly here. (i) Dermal thickness in the treated mice. The dermal thickness of LAP-treated mice was reduced compared with that of PBS-treated control mice. There was no statistically significant dose dependency of inhibition in the LAP group. [LAP (50 ng): 204.0 ± 19.70 μm vs PBS: 269.4 ± 48.43 μm, $P = 0.025$, LAP (500 ng): 176.5 ± 28.20 μm vs PBS: 269.4 ± 48.43 μm, $P = 0.014$].

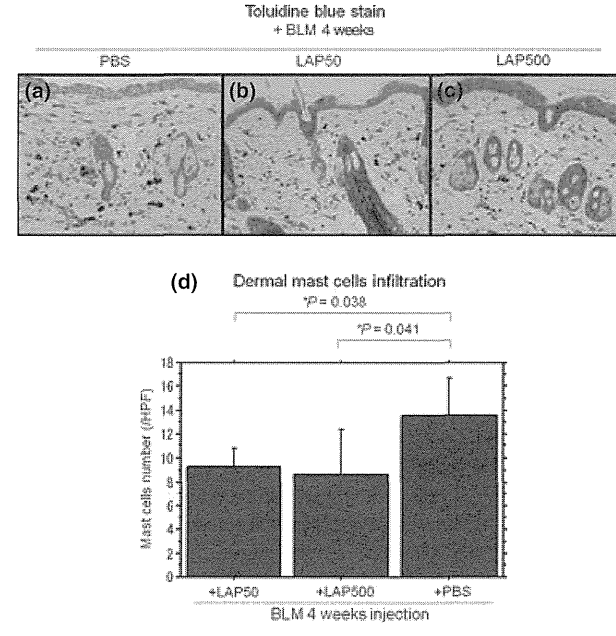

Figure 2. Toluidine blue staining showing mast cell infiltration after bleomycin (BLM)/latency-associated peptide (LAP) treatment. (a) Dermal infiltration of mast cells after injection of BLM (500 μg/ml) and PBS for 4 weeks as a control. (b, c) Histopathological changes in mast cell infiltration. LAP-treated group showed a decrease compared with control group. (d) Dermal mast cell number. Dermal mast cell number was decreased in the LAP treatment group. However, there was no significant dose dependency of inhibition in the LAP group. [LAP (50 ng): 9.25 ± 1.52/HPF vs PBS: 13.60 ± 3.09/HPF, $P = 0.041$, LAP (500 ng): 8.66 ± 3.66/HPF vs PBS: 13.60 ± 3.09/HPF, $P = 0.038$].